Journal of Organometallic Chemistry 694 (2009) 3076–3083

Contents lists available at ScienceDirect

Journal of Organometallic Chemistry

journal homepage: www.elsevier.com/locate/jorganchem

Chemical structure–stereospecificity relationship of internal donor in heterogeneous Ziegler–Natta catalyst for propylene polymerization by DFT and MM calculations

Jin Woo Lee, Won Ho Jo *

Department of Materials Science and Engineering, Seoul National University, Seoul 151-742, Republic of Korea

ARTICLE INFO

Article history:
Received 11 February 2009
Received in revised form 20 May 2009
Accepted 21 May 2009
Available online 27 May 2009

Keywords:
Density functional theory
Molecular mechanics
Ziegler–Natta catalyst
Isotactic polypropylene
Internal donor
1,3-Diether

ABSTRACT

The effect of chemical structure of 2,2′-disubstituted 1,3-dimethoxypropane (so-called 1,3-diether) on the performance of Ziegler–Natta (ZN) catalyst was investigated by using density functional theory and molecular mechanics. Calculation of the energy barrier during insertion of propylene reveals that the isospecific active site created on the (1 0 0) surface of $MgCl_2$ is more active than the aspecific active site created on the (1 1 0) surface of $MgCl_2$ for propylene polymerization. When the adsorption energies of various 1,3-diethers are calculated and analyzed in terms of isotacticity, it is found that the isotacticity of polypropylene increases as 1,3-diether is adsorbed more preferentially on the (1 1 0) surface. Since analysis of energetics for insertion of propylene into the active site created on the (1 1 0) surface with 1,3-diether coordinated to Mg atom in the vicinity of the active site reveals that the coordination of 1,3-diether does not transform the aspecific active site on the (1 1 0) surface into isospecific one, it is concluded that the primary function of 1,3-diether is to prevent the formation of aspecific site on the (1 1 0) surface, without significant decrease in the number of the isospecific active site created on the (1 0 0) surface. A systematic analysis of various model compounds for 1,3-diether suggests that the substitution of highly branched hydrocarbon at the C_2 position of 1,3-diether results in better performance of ZN catalyst.

1. Introduction

It has been known that internal (or external) donors, as added to $MgCl_2$-supported heterogeneous Ziegler–Natta (ZN) catalyst, improve both the isotacticity and the productivity of polypropylene [1–4]. However, the mechanism underlying the role of donor has not been completely understood, although many experimental [5–17] and theoretical [18–33] studies have been reported. A thorough understanding of the relationship between the chemical structure of donor and the isotacticity (and productivity) of polypropylene are essential for molecular design of better donor to yield highly isotactic polypropylene with high productivity.

A systematic density functional theory (DFT) study has suggested that $TiCl_3$ molecules can easily coordinate onto the (1 0 0) surface of $MgCl_2$, resulting in the formation of polynuclear species [28]. Moreover, Corradini et al. [28,29] have suggested that these polynuclear sites would be highly isospecific because of a close resemblance to the C_2 symmetric site that has been proposed to be isospecific from the molecular mechanics (MM) study on $TiCl_3$-based catalytic system [27]. Indeed, our recent DFT calculation has demonstrated that the active site created by Ti_2Cl_7 adsorption on the (1 0 0) surface of $MgCl_2$ is highly isospecific [30]. On the other hand, it has been reported that a stable active site is formed by epitactical adsorption of $TiCl_4$ (or $TiCl_3$ after reduction) on the (1 1 0) surface, which results in an aspecific active site [21,28]. Accordingly, it has been suggested that the primary function of donor is to suppress the formation of aspecific active site by preferential coordination of donor onto the (1 1 0) surface of $MgCl_2$ [20].

Other models have suggested that the location of donors in the vicinity of active sites is prerequisite for the formation of isospecific active sites: the donor converts aspecific site into isospecific one by creating suitable chiral environment. High-resolution ^{13}C NMR study has suggested that the stereoblock nature of polypropylene (mixture of highly isotactic, weakly isotactic and syndiotactic sequences) is related to reversible change in the steric environment of active sites, which is associated with the presence of donor in the vicinity of active site [8]. Recently, Correa et al. [25] have proposed a possible active site where steric environment is conditioned depending on the adsorption of donor.

Although those studies have provided significant knowledge on the structure of the isospecific active site and the role of donor, a complete agreement has not been made because the stability of active site is still controversial and a definite evidence for the presence

* Corresponding author. Tel.: +82 2 880 7192; fax: +82 2 885 1748.
E-mail address: whjpoly@snu.ac.kr (W.H. Jo).

0022-328X/$ - see front matter © 2009 Elsevier B.V. All rights reserved.
doi:10.1016/j.jorganchem.2009.05.030

or the absence of donor in the neighborhood of isospecific active site has not been reported. Recently, an experimental and theoretical Raman spectroscopy study has reported that an active site created by the adsorption of $TiCl_4$ on the (1 1 0) surface of $MgCl_2$ is stable whereas an active site created by the adsorption of Ti_2Cl_8 on the (1 0 0) surface of $MgCl_2$ is unstable [31]. On the other hand, an X-ray structure analysis [6] and a systematic DFT study [28] have suggested that $TiCl_4$ is adsorbed on the (1 0 0) surface of $MgCl_2$ with the formation of dimeric Ti_2Cl_8 species. Furthermore, since the effect of chemical structure of donor on the isotacticity and the productivity of polypropylene has not been completely elucidated, the development of industrial catalyst has been achieved experimentally by trial and error. Hence, computational approach as an alternative method may provide us with more detailed information at a molecular level. The primary objective of this study is to establish the relationship between the chemical structure of internal donor and the isotacticity (and productivity) of polypropylene by using DFT and MM calculations. For this purpose, the polymerization kinetics of propylene at the active sites created on the (1 1 0) and the (1 0 0) surfaces of $MgCl_2$ were compared with each other, and the adsorption energies of various 2,2′-disubstituted 1,3-dimethoxypropanes (so-called 1,3-diethers) on both surfaces of $MgCl_2$ were calculated and analyzed in terms of isotacticity, where 1,3-diethers are known to be good internal donors due to their good chemical stability toward cocatalyst. The stereoselectivity of the active site created on the (1 1 0) surface with 1,3-diether coordinated to Mg atom in the vicinity of the active site is also examined. Based on these simulation results, a guideline for rational design of better internal donor is proposed.

2. Computational details

All DFT calculations were performed using the VWN functional [34] corrected by the exchange functional of Becke [35] and the correlation functional of Perdew [36] in the Amsterdam Density Functional package [37]. The electronic configurations were described by the triple-ζ Slater type orbital basis set for Ti, O and double-ζ basis set for Mg, Cl, C and H with a single polarization function for all atoms. The frozen-cores used for DFT calculation are [Ar] for Ti, [Ne] for Mg and Cl, [He] for C and O.

The MM calculations have been performed by using the universal force field [38]. The activation energy for the adsorption of 1,3-diether on the (1 1 0) and the (1 0 0) surfaces of $MgCl_2$ was calculated by means of conformer search in *Cerius*^{2}.

To calculate the energetics for insertion of propylene into the active site created on the (1 1 0) surface with or without 1,3-diether coordinated at Mg atom in the vicinity of the active site, two model clusters of Mg_8Cl_{16} were used for $MgCl_2$. The Mg–Cl distance and the Cl–Mg–Cl angle in the cluster were fixed to 2.49 Å and 90°, respectively. These cluster structures are nearly equal to the $MgCl_2$ crystal in the bulk [39]. The insertion of propylene follows the Cossee–Arlman mechanism [40–42] revised by Brookhart and Green [43], where the distance between the incoming propylene and the α-carbon of the growing chain (i.e., the carbon which is directly attached to the titanium) is taken as the reaction coordinate. Propylene monomer is inserted by the manner of decreasing the reaction coordinate stepwise, where full optimization of geometry is performed with respect to all other degrees of freedom at each step. Because of the presence of a Ti(III) atom, unrestricted DFT calculations were performed.

To investigate the interaction between $MgCl_2$ surface and 1,3-diether, both DFT and MM calculations have been carried out by using model clusters of Mg_6Cl_{12} and Mg_7Cl_{14} for (1 1 0) and (1 0 0) surfaces of $MgCl_2$, respectively. Geometries of adsorbed donor molecules have always been fully optimized, while the Mg–Cl distance and the Cl–Mg–Cl angle in the cluster were fixed as described above. The adsorption energy of 1,3-diether, E, is calculated by the difference between the total energy ($E_{D/S}$) of the structure formed by adsorption of a 1,3-diether (D) on a model cluster for $MgCl_2$ (S) and the sum of the electronic energies of a free 1,3-diether ($E_{D,f}$) and the model cluster ($E_{S,f}$): $E = E_{D/S} - E_{D,f} - E_{S,f}$. This adsorption energy can be decomposed into the intramolecular energy (E_{intra}) required to deform a free 1,3-diether suitable for adsorption on the model cluster and the inter-molecular energy (E_{inter}) between the deformed 1,3-diether and the model cluster as follows:

$$E = E_{intra} + E_{inter}$$
$$E_{intra} = E_D - E_{D,f}$$
$$E_{inter} = E_{D/S} - E_D - E_{S,f}$$

where E_D is the potential energy of the deformed 1,3-diether. By definition, the values of E and E_{inter} are always negative, whereas the value of E_{intra} is always positive.

3. Results and discussion

3.1. Polymerization kinetics of propylene at isospecific and aspecific active sites

For propylene insertion into a catalytic site, the catalytic site should be first activated by a cocatalyst, leading to the formation of Ti–alkyl bond by replacement of one dangling Cl coordinated to Ti by an alkyl chain. Fig. 1 represents two types of intermediate states during insertion of propylene into the active site **1** created by $TiCl_3$ adsorption on the (1 1 0) surface of $MgCl_2$, where one dangling Cl atom is replaced by an isobutyl group. When a propylene monomer is coordinated to the active site **1**, leading to a π-complex (**C1**$_{re}$ and **C1**$_{si}$ in Fig. 1), it is observed that the C=C bond of propylene monomer is perpendicular to the Ti–C_α bond and the growing chain is stabilized by β–agostic interaction, as evidenced by the elongated C_β–H_β bond length (1.14 Å) as compared with the normal C–H bond length (1.10 Å). When a propylene monomer approaches the active site, we assume that the growing chain is rotated to the opposite side of methyl group of the inserting propylene, leading to the insertion of propylene into the Ti–isobutyl bond through the transition state (**T1**$_{re}$ and **T1**$_{si}$ in Fig. 1) stabilized by a remarkable α–agostic interaction (note that the C_α–H_α distance is 1.14 Å). This assumption is supported by a previous study which reports that ethylene insertion through the transition state stabilized by α–agostic interaction is energetically more favorable than that through the transition state stabilized by β–agostic interaction [44]. The final product (**P1**$_{re}$ and **P1**$_{si}$ in Fig. 1) shows a strong β–agostic interaction by which the C_β–H_β distances for *re*- and *si*-insertion become 1.15 and 1.16 Å, respectively. This active site is aspecific because not only the enthalpies of formation of π-complex for *re*- and *si*-insertion are similar (−12.6 and −11.7 kcal/mol for *re*- and *si*-insertion, respectively) but also the activation energies of *re*- and *si*-insertion are comparable with each other (10.3 and 10.0 kcal/mol for *re*- and *si*-insertion, respectively), as listed in Table 1.

As mentioned above, the π-complex formed at the active site **1** is stabilized by strong β–agostic interaction, but this β–agostic interaction should be broken and switched to weak α–agostic interaction to facilitate the insertion of propylene. On the other hand, both of the π-complex and the transition state at the active site **2** created by Ti_2Cl_7 adsorption on the (1 0 0) surface, which was proved to be a highly isospecific active site, are stabilized by weak α–agostic interaction, and hence the reorientation of growing chain is not required for insertion of propylene [30]. This implies that the insertion of propylene into the active site **1** should

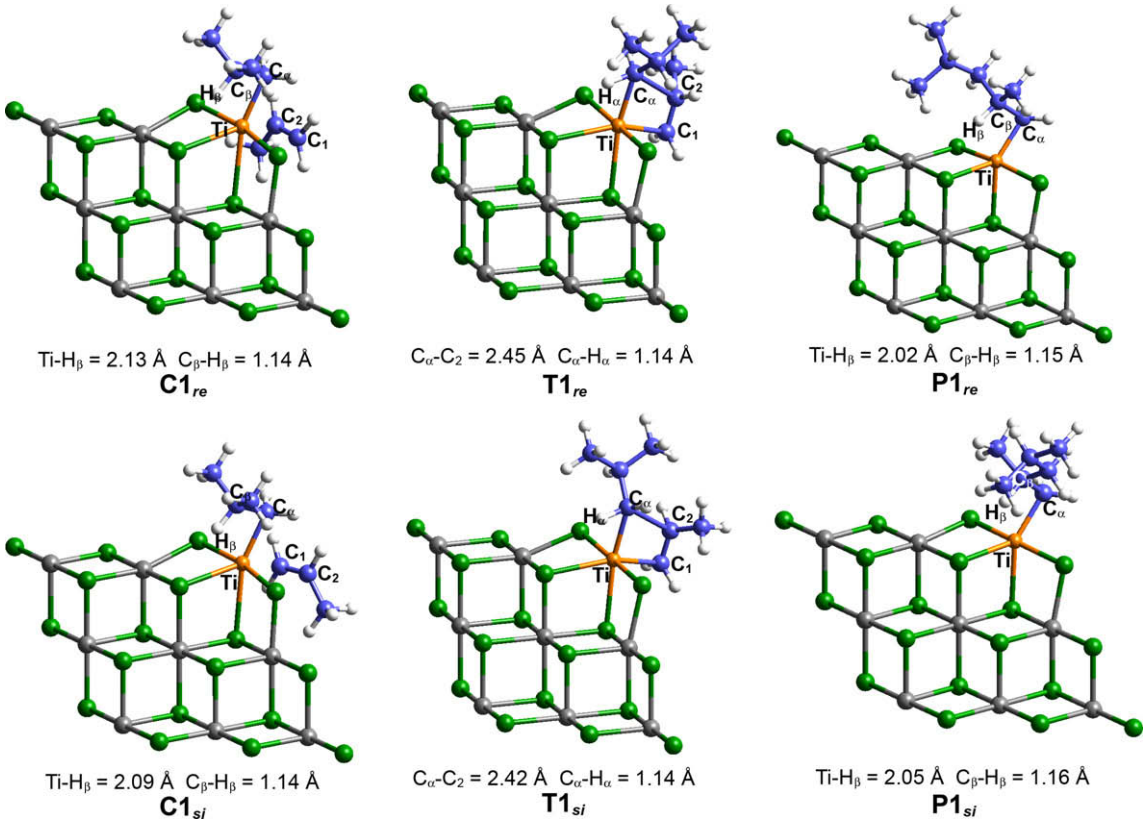

Fig. 1. DFT optimized structures of π-complex (**C1**$_{re}$ and **C1**$_{si}$), transition state (**T1**$_{re}$ and **T1**$_{si}$) and product (**P1**$_{re}$ and **P1**$_{si}$) for propylene insertion into the active site **1** for *re*- and *si*-insertion. Mg and Cl atoms are represented by grey ball and green ball in model cluster, respectively. (For interpretation of the references to colour in this figure legend, the reader is referred to the web version of this article.)

Table 1
Energetics for propylene insertion into the active site **1** and **1′**.[a]

Active site	Enantioface	π-Complex[b]	Transition state[c]	Product[d]
1	*re*	−12.6	−2.3	−19.9
1	*si*	−11.7	−1.7	−18.9
1′	*re*	−9.0	2.9	−18.3
1′	*si*	−8.8	3.1	−19.3

[a] Energies in kcal/mol.
[b] Relative energy of π-complex with respect to the sum of the energies of a separated monomer and an active site.
[c] Relative energy of transition state with respect to the sum of the energies of a separated monomer and an active site.
[d] Relative energy of product with respect to the sum of the energies of a separated monomer and an active site.

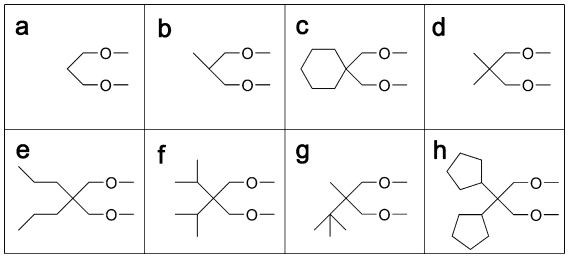

Fig. 2. Chemical structure of various 1,3-diethers studied in this paper to establish the relationship between the chemical structure of internal donor and the isotacticity (and productivity) of polypropylene.

overcome higher energy barrier (10.0 kcal/mol) as compared with the insertion into the active site **2** (5.8 kcal/mol). This result leads us to assume that the polymerization kinetics of propylene at the isospecific active site **2** created on the (1 0 0) surface is much faster than that at the aspecific active site **1**, which has been supported by recent experimental studies [13–15], where the propagation rate constant at an isospecific active site is several times lager than that at an aspecific active site. It is also noteworthy that the calculated activation energies of 10.0 and 5.8 kcal/mol are in a good agreement with an experimental value (6.8 ∼ 9.1 kcal/mol) [45].

3.2. The role of 1,3-diether

The effect of 1,3-diether on the distribution of isospecific and aspecific active sites, which is closely related with the isotacticity and the productivity of polypropylene, was investigated by using DFT and MM calculations. For comparison with experiment, eight different 1,3-diethers were chosen as internal donors for our theoretical analysis, because their structural effect on the isotacticity of polypropylene was experimentally reported [18,20]. The chemical structures of 1,3-diethers studied in this paper are represented in Fig. 2. Before the adsorption energy of 1,3-diether on the surface of $MgCl_2$ was calculated, the conformational energy of 1,3-dimethoxypropane (a in Fig. 2) at the free state was first calculated as functions of two dihedral angles defined by the rotation around C_1–C_2 and C_2–C_3 bonds, as shown in Fig. 3. DFT calculation shows that 1,3-dimethoxypropane has four conformational minima corresponding to (TT), (TG^+), (G^+G^+) and (G^+G^-) or their equivalents. The calculation also shows that (G^+G^+) has the lowest conformational energy while (G^+G^-) does the highest conformational energy and that the energy difference between (G^+G^+) and (G^+G^-) is *ca.* 3 kcal/mol. When the conformational energies of all other 1,3-diethers represented in Fig. 2 are calculated, it is realized that

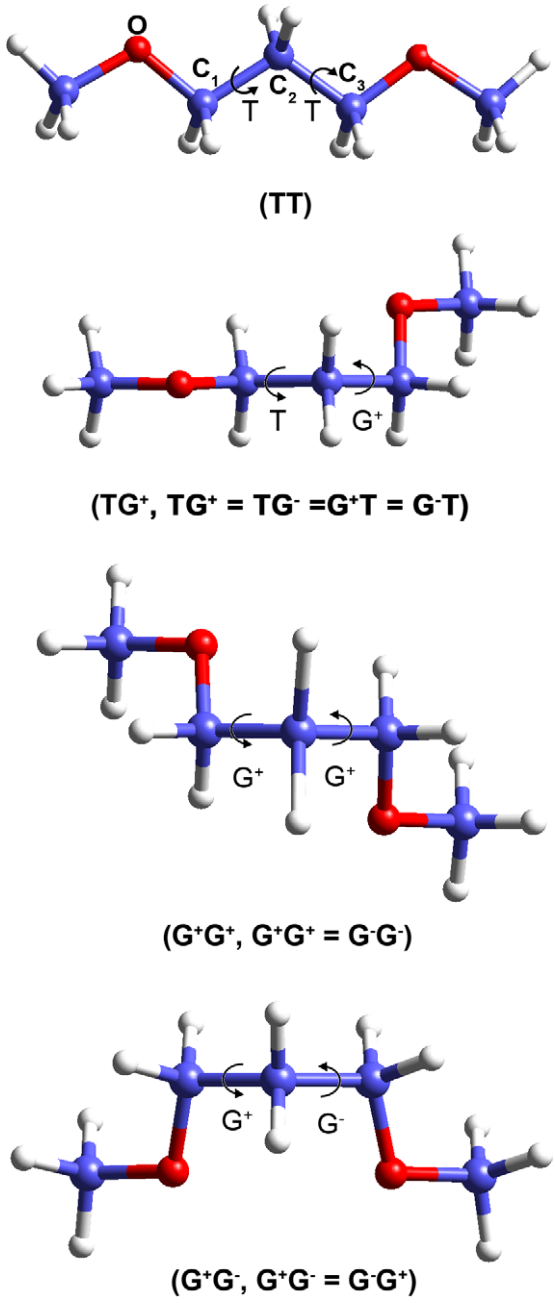

Fig. 3. DFT optimized structures of 1,3-dimethoxypropane at four energy minima. Each conformation has 1, 4, 2 and 2 conformational degeneracy, respectively.

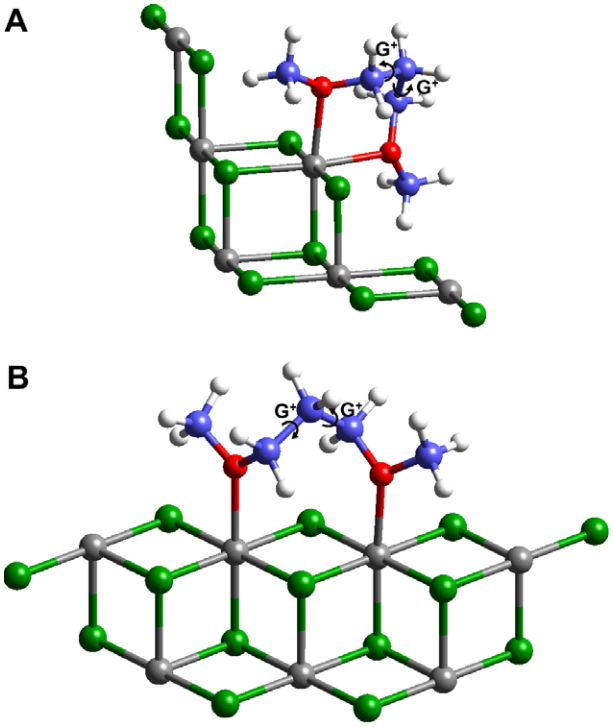

Fig. 4. DFT optimized structures of 1,3-dimethoxypropane adsorbed on the (1 1 0) surface (A) and on the (1 0 0) surface (B) of $MgCl_2$ in (G^+G^+) conformation. Mg and Cl atoms are represented by grey ball and green ball in model cluster, respectively. (For interpretation of the references to colour in this figure legend, the reader is referred to the web version of this article.)

all 1,3-diethers show the same behavior as 1,3-dimethoxypropane. Scordamaglia and Barino [18] also calculated the most probable conformation of various 1,3-diethers using the Conformations' Statistical Distribution method, and their calculations are in a good agreement with our results. Hence, it is reasonable to assume that the 1,3-diethers are in the (G^+G^+) conformation when they are adsorbed on the surface of $MgCl_2$ in this study. The DFT optimized geometries of 1,3-dimethoxypropane adsorbed on the (1 1 0) and the (1 0 0) surface of $MgCl_2$ are shown in Fig. 4. All other 1,3-diethers are also adsorbed by the same manner. Only the most stable coordination mode (chelate coordination) is considered on the (1 1 0) surface in this study.

When the adsorption energy, *E*, was calculated by using DFT, it was found that all 1,3-diethers were adsorbed more strongly on the (1 1 0) surface than the (1 0 0) surface of $MgCl_2$ (Table 2). When the basis set superposition error (BSSE) was calculated for the adsorption of a, b and c in Fig. 2 on both surfaces, it is realized that the BSSEs are *ca.* 4.4 kcal/mol for all cases and this value is negligibly small as compared with the adsorption energy. Therefore, we assumed that the BSSE does not affect the adsorption behavior of 1,3-diethers. For this reason, the effect of the BSSE was not taken into account in this study.

Since the adsorption of 1,3-diether on both surfaces of $MgCl_2$ is strongly exothermic, as can be realized from the value of *E* in Table 2, the desorption of 1,3-diether becomes energetically disfavored and therefore the adsorption is effectively irreversible. Under this condition, it is expected that the selective adsorption of 1,3-diether on one of two surfaces of $MgCl_2$ is governed by the activation energy for adsorption. For this reason, the activation energy for adsorption on the (1 1 0) and (1 0 0) surface of $MgCl_2$ was calculated by the manner of rotating two methoxy groups of 1,3-diether stepwise from the trans state to the conformation for adsorption, where full optimization of geometry is performed at each step with respect to all other degrees of freedom. The activation energy calculated by MM shows that the adsorption of 1,3-diether on the (1 1 0) surface is a barrierless process because the large rotation of methoxy group is not necessary (Fig. 4A), while the adsorption on the (1 0 0) surface undergoes an energy barrier because 1,3-diether should suffer a large conformational change (Fig. 4B). Table 3 shows that the isotacticity of polypropylene reported in experimental works [18,20] increases from 64.9% to 97.5% as the activation energy for the adsorption of 1,3-diether on the (1 0 0) surface ($E_a^{(100)}$) increases from 0.5 to 4.1 kcal/mol, indicating that the isotacticity of polypropylene increases as 1,3-diether is adsorbed more preferentially on the (1 1 0) surface.

To investigate the effect of adsorbed 1,3-diether on the stereospecificity of the active site created on the (1 1 0) surface of $MgCl_2$,

Table 2
Comparison of adsorption energies of 1,3-diethers represented in Fig. 2 on the (1 1 0) and (1 0 0) surfaces of $MgCl_2$ in (G+G$^+$) conformation by DFT calculation.[a]

Donor	(1 1 0) Surface			(1 0 0) Surface			ΔE[b]	ΔE_{intra}[c]	ΔE_{inter}[d]
	E	E_{intra}	E_{inter}	E	E_{intra}	E_{inter}			
a	−28.6	7.1	−35.7	−25.8	4.7	−30.5	2.8	−2.4	5.2
b	−29.4	6.8	−36.2	−24.9	5.8	−30.7	4.5	−1.0	5.5
c	−29.9	6.4	−36.3	−22.0	8.2	−30.2	7.9	1.8	6.1
d	−29.3	6.1	−35.4	−22.7	7.3	−30.0	6.6	1.2	5.4
e	−30.9	5.8	−36.7	−21.8	8.6	−30.4	9.1	2.8	6.3
f	−29.4	8.2	−37.6	−17.8	12.5	−30.3	11.6	4.3	7.3
g	−30.7	6.2	−36.9	−18.9	10.7	−29.6	11.8	4.5	7.3
h	−30.5	6.8	−37.3	−17.9	12.2	−30.1	12.6	5.4	7.2

[a] Energies in kcal/mol.
[b] $\Delta E = E^{(100)} - E^{(110)}$.
[c] $\Delta E_{intra} = E_{intra}^{(100)} - E_{intra}^{(110)}$.
[d] $\Delta E_{inter} = E_{inter}^{(100)} - E_{inter}^{(110)}$.

Table 3
Activation energies for adsorption of 1,3-diethers represented in Fig. 2 on the (1 0 0) surface of $MgCl_2$ ($E_a^{(100)}$) by MM calculation.[a]

Donor	$E_a^{(100)}$	Isotactic index (%)[b]
a	0.5	64.9
b	0.9	74.9
c	1.7	87.7
d	1.7	89.8
e	2.2	93.6
f	2.5	95.4
g	4.1	95.8
h	3.9	97.5

[a] Energies in kcal/mol.
[b] Taken from Refs. [18,20].

we performed calculation for insertion of propylene into the active site **1**′, where 2-methyl-1,3-dimethoxypropane (b in Fig. 2) was beforehand coordinated to the nearest Mg atom from the active site. The intermediate states during insertion of propylene into the active site **1**′ are similar to those into the active site **1**. As shown in Fig. 5, since a donor molecule coordinated to the (1 1 0) surface is far apart from a growing chain, it does not interact repulsively with the growing chain during insertion of propylene. Consequently, both the enthalpy of formation of π-complex and the activation energy for *re*-insertion are nearly the same as those for *si*-insertion (−9.0 and −8.8 kcal/mol for the enthalpy of π-complex formation for *re*- and *si*-insertion, respectively; 11.9 kcal/mol for the activation energy for both *re*- and *si*-insertion). Furthermore, since the activation energies during insertion of propylene into the active site **1**′ are very similar to those into the active site **1** (Table 1), the coordination of 1,3-diether does not transform the aspecific active site created on the (1 1 0) surface into isospecific one and therefore does not affect the polymerization kinetics of this site. This leads us to conclude that the primary function of 1,3-diether is to prevent the creation of the aspecific active site **1** on

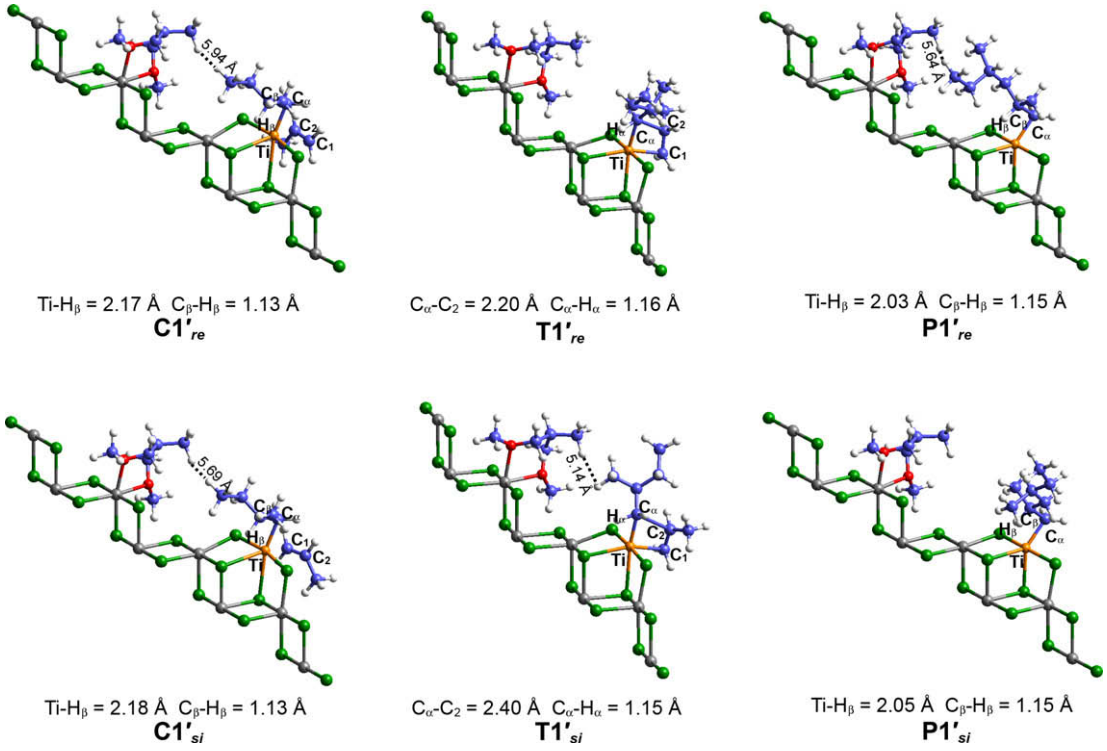

Fig. 5. DFT optimized structures of π-complex (**C1**′$_{re}$ and **C1**′$_{si}$), transition state (**T1**′$_{re}$ and **T1**′$_{si}$) and product (**P1**′$_{re}$ and **P1**′$_{si}$) for propylene insertion into the active site **1**′ for *re*- and *si*-insertion. Mg and Cl atoms are represented by grey ball and green ball in model cluster, respectively. (For interpretation of the references to colour in this figure legend, the reader is referred to the web version of this article.)

the (1 1 0) surface without significant decrease in the number of the isospecific active site on the (1 0 0) surface by selectively poisoning the (1 1 0) surface of $MgCl_2$, which is consistent with experimental results [13] showing that the number of total active sites is significantly reduced while the number of isospecific active sites is only slightly altered when 1,3-diether is used as an internal donor. As a result, an addition of 1,3-diether improves not only the isotacticity but also the catalytic activity (kg of PP/g of Ti·hour). Our calculation predicts that the (1 0 0) surface starts to be blocked by internal donor as the concentration of internal donor exceeds a critical value. As a consequence, the number of the isospecific active site **2** will be reduced, resulting in the decrease of isotacticity and productivity. This prediction can successfully explain an experimental result [9] that the isotacticity and productivity increase first and then decrease as the concentration of internal donor increases, showing a maximum at the critical concentration.

Recently, Correa et al. [25] has suggested that diesters can be adsorbed on the (1 1 0) surface in various coordination modes and that the aspecific active site **1** can be converted into highly isospecific active site when diesters such as succinates are coordinated on both sides of the isolated Ti species in bridge coordination mode. However, they have also reported that diesters are adsorbed less preferentially on the (1 1 0) surface than 1,3-diethers and therefore a large amount of diesters can be adsorbed on the (1 0 0) surface. Accordingly, it is expected that the ZN catalyst with diester is less active than the ZN catalyst with diether, because diester may block the (1 0 0) surface where the highly active and isospecific site can be created.

3.3. The effect of chemical structure on the selective adsorption of 1,3-diether on the (1 1 0) surface

It is worth noting that the adsorption energy of 1,3-diether on the (1 1 0) surface is almost the same ($-28.6 \sim -30.9$ kcal/mol) for all 1,3-diethers, while the adsorption energy on the (1 0 0) surface decreases from -25.8 to -17.8 kcal/mol as the bulkiness of the substituent at the C_2 position in 1,3-diether increases (Table 2). As a result, the adsorption energy difference between the (1 0 0) and (1 1 0) surfaces, $\Delta E = (E^{(100)} - E^{(110)})$, increases from 2.8 to 12.6 kcal/mol as the size of substituent increases from hydrogen to cyclopentyl group (Table 2). In order to establish the relationship between the chemical structure and the selective adsorption of 1,3-diether on the (1 1 0) surface, the adsorption energy is decomposed into the intra- and inter-molecular energy terms: E_{intra} (conformational energy of 1,3-diether) and E_{inter} (interaction energy between 1,3-diether and $MgCl_2$). Here, it is noted that the decrease of the adsorption energy on the (1 0 0) surface due to an increase in bulkiness of C_2 substituent arises mainly from the increase of E_{intra}, as can be seen in Table 2. For an example, when a 1,3-diether (g in Fig. 2) is adsorbed on the (1 0 0) surface, two methoxy groups of the 1,3-diether should be rotated from trans to gauche conformation (defined by the dihedral angle of C–C–O–C) to facilitate the attractive electrostatic interaction between oxygen of 1,3-diether and Mg atom of $MgCl_2$, as illustrated in Fig. 6. However, this conformational change causes a repulsive interaction between methoxy group and the substituent at the C_2 position to increase. Therefore, it is easily expected that the intramolecular energy of a 1,3-diether as adsorbed on the (1 0 0) surface increases with increasing the bulkiness of substituent. On the other hand, a large conformational change is not necessary when a 1,3-diether is adsorbed on the (1 1 0) surface, as illustrated in Fig. 4A, and therefore the conformational energies (E_{intra}) are nearly the same regardless of the bulkiness of substituent. Consequently, ΔE strongly depends on $\Delta E_{intra}\left(= \Delta E_{intra}^{(100)} - \Delta E_{intra}^{(110)}\right)$ rather than $\Delta E_{inter}\left(= \Delta E_{inter}^{(100)} - \Delta E_{inter}^{(110)}\right)$.

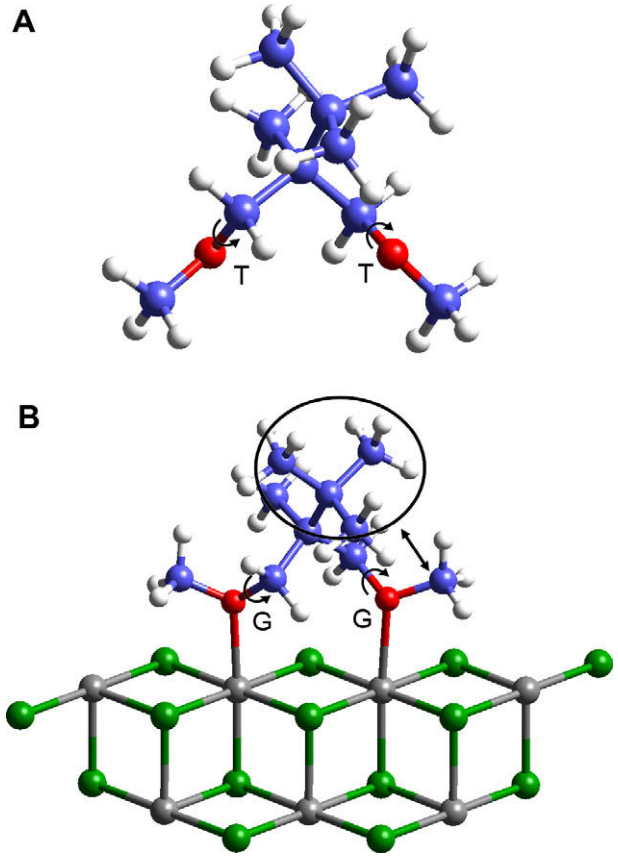

Fig. 6. Conformational change of 2-methyl-2′-*t*-butyl-1,3-dimethoxypropane by adsorption on the (1 0 0) surface of $MgCl_2$. The conformational change from the *trans* conformation at the free state (A) to the gauche conformation at adsorbed state (B) is represented, where the dihedral angle is defined by the rotation around the C–O bond. Mg and Cl atoms are represented by grey ball and green ball in model cluster, respectively. (For interpretation of the references to colour in this figure legend, the reader is referred to the web version of this article.)

The activation energy for adsorption of 1,3-diether on the (1 0 0) surface ($E_a^{(100)}$) also increases from 0.5 to 4.1 kcal/mol as the bulkiness of substituent increases, as can be seen in Table 3. It is noteworthy that ΔE (Table 2) is closely correlated to $E_a^{(100)}$ (Table 3). This is easily rationalized because the increase of both ΔE and $E_a^{(100)}$ with the bulkiness of substituent arises from the repulsive interaction between methoxy groups and substituents at the C_2 position. Therefore, although the adsorption of 1,3-diether on the surface of $MgCl_2$ is kinetically controlled, the selective adsorption of 1,3-diether on the (1 1 0) surface can be simply evaluated from ΔE. Consequently, it is reasonable to conclude that the chemical structure (the bulkiness and shape of substituent) of 1,3-diether is the most important factor for controlling the selective adsorption of 1,3-diether on the (1 1 0) surface of $MgCl_2$.

To search a chemical structure of 1,3-diether for more selective adsorption on the (1 1 0) surface, the adsorption energies of 13 different model compounds for 1,3-diether represented in Fig. 7 were calculated by using DFT, as listed in Table 4, and compared with each other. Because it is realized from Table 2 that the substitution of *t*-butyl group at C_2 position of 1,3-diether (g in Fig. 2) significantly increases the adsorption energy difference (ΔE), the model compounds for 1,3-diether were designed to have a *t*-butyl group (**1**–**7** in Fig. 7) or neopentyl group (**1′**–**7′** in Fig. 7) at one substitution at the C_2 position, while the other substitution at the C_2 position varies from methyl to 3,3′-dimethylbutyl group. When the adsorption energy differences of all model compounds for 1,3-diether are compared with each other, it reveals that the substitution of

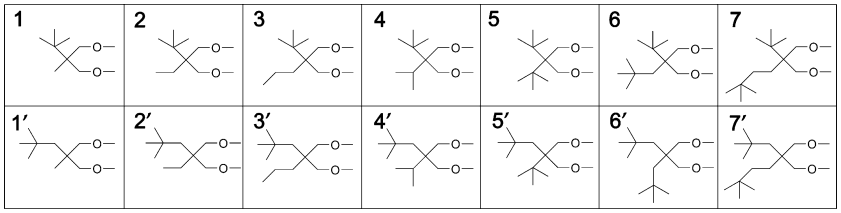

Fig. 7. Model compounds for 1,3-diether as internal donor.

Table 4
Comparison of adsorption energies of 1,3-diethers represented in Fig. 7 on the (1 1 0) and (1 0 0) surfaces of $MgCl_2$ in (G^+G^+) conformation by DFT calculation.[a]

Donor	(1 1 0) Surface			(1 0 0) Surface			ΔE[b]	ΔE_{intra}[c]	ΔE_{inter}[d]
	E	E_{intra}	E_{inter}	E	E_{intra}	E_{inter}			
1	−30.7	6.2	−36.9	−18.9	10.7	−29.6	11.8	4.5	7.3
2	−31.4	6.2	−37.6	−17.7	11.6	−29.3	13.7	5.4	8.3
3	−31.4	6.1	−37.5	−17.8	11.3	−29.1	13.6	5.2	8.4
4	−28.0	8.7	−36.7	−13.6	16.1	−29.7	14.4	7.4	8.0
5	−27.5	9.1	−36.6	−9.2	18.6	−27.8	18.3	9.5	8.8
6	−30.1	6.5	−36.6	−15.1	13.1	−28.2	15.0	6.6	8.4
7	−31.7	7.6	−39.3	−17.7	11.9	−29.6	14.0	4.3	9.7
1′	−29.5	7.4	−36.9	−18.5	11.3	−29.8	11.0	3.9	7.1
2′	−30.1	6.4	−36.5	−18.5	11.6	−30.1	11.6	5.2	6.4
3′	−30.2	6.3	−36.5	−18.6	11.6	−30.2	11.6	5.3	6.3
4′	−29.7	7.0	−36.7	−17.5	12.5	−30.0	12.2	5.5	6.7
5′	−30.1	6.5	−36.6	−15.1	13.1	−28.2	15.0	6.6	8.4
6′	−27.1	7.9	−35.0	−14.3	15.7	−30.0	12.8	7.8	5.0
7′	−31.1	7.5	−38.6	−18.1	12.1	−30.2	13.0	4.6	8.4

[a] Energies in kcal/mol.
[b] $\Delta E = E^{(100)} - E^{(110)}$.
[c] $\Delta E_{intra} = E^{(100)}_{intra} - E^{(110)}_{intra}$.
[d] $\Delta E_{inter} = E^{(100)}_{inter} - E^{(110)}_{inter}$.

branched hydrocarbons (e.g., *t*-butyl and neopentyl) induces larger ΔE than does the substitution of linear hydrocarbons (e.g., methyl, ethyl and propyl), as can be seen in Table 4. Particularly, the value of ΔE of **5** (disubstitution of *t*-butyl) is 18.3 kcal/mol, which is considerably higher than the values (see Table 2) of commercial 1,3-diethers (a–h in Fig. 2). The value of ΔE increases first and then decreases as the bulkiness of the second substituent increases from methyl to 3,3′-dimethylbutyl, showing a maximum at the substitution of *t*-butyl group for both cases of *t*-butyl- and neopentyl-based 1,3-diethers (Table 4). Another interesting feature is that the values of ΔE of *t*-butyl-based 1,3-diethers are always higher than those of neopentyl-based 1,3-diethers by *ca.* 2 kcal/mol when the second substituent at the C_2 position is the same. This result leads us to conclude that the substitution of highly branched hydrocarbon such as *t*-butyl group is the most effective for better isotacticity and productivity.

4. Conclusions

In this study, the effect of the chemical structure of 1,3-diether on the performance of ZN catalyst was investigated. DFT and MM calculations reveal that the isotacticity and the productivity of polypropylene increase as 1,3-diether is adsorbed more preferentially on the (1 1 0) surface. Calculation also reveals that diether does not transform the aspecific active site created on the (1 1 0) surface into an isospecific one, indicating that the primary function of 1,3-diether, as an internal donor, is to increase the relative concentration of isospecific active site created on the (1 0 0) surface by selective adsorption of 1,3-diether on the (1 1 0) surface, resulting in improvement of the isotacticity and the productivity of polypropylene. 1,3-Diether is adsorbed more preferentially on the (1 1 0) surface as the substituent at the C_2 position of 1,3-diether becomes bulkier, because the activation energy required to deform a free 1,3-diether suitable for the adsorption on the (1 0 0) surface increases.

A systematic analysis of the adsorption energy of various model compounds for 1,3-diether on the (1 1 0) and (1 0 0) surfaces of $MgCl_2$ reveals that the substitution of highly branched hydrocarbon at the C_2 position of 1,3-diether increases the adsorption energy difference (ΔE) as compared with the substitution of linear hydrocarbons, indicating that the substitution of highly branched hydrocarbons is more effective for better isotacticity and productivity.

Acknowledgement

The authors thank the Ministry of Education, Science and Technology (MEST), Korea for financial support through the Global Research Laboratory (GRL) program.

References

[1] P.C. Barbè, G. Cecchin, L. Noristi, Adv. Polym. Sci. 81 (1986) 1–81.
[2] M.C. Sacchi, I. Tritto, P. Locatelli, Prog. Polym. Sci. 16 (1991) 331–360.
[3] M.C. Sacchi, I. Tritto, C. Shan, R. Mendichi, L. Noristi, Macromolecules 24 (1991) 6823–6826.
[4] E. Albizzati, U. Giannini, G. Morini, M. Galimberti, L. Barino, R. Scordamaglia, Macromol. Symp. 89 (1995) 73–89.
[5] G. Morini, E. Albizzati, G. Balbontin, I. Mingozzi, M.C. Sacchi, F. Forlini, I. Tritto, Macromolecules 29 (1996) 5770–5776.
[6] A.G. Potapov, V.V. Kriventsov, D.I. Kochubey, G.D. Bukatov, V.A. Zakharov, Macromol. Chem. Phys. 198 (1997) 3477–3484.
[7] V. Busico, R. Cipullo, G. Talarico, A.L. Segre, J.C. Chadwick, Macromolecules 30 (1997) 4786–4790.
[8] V. Busico, R. Cipullo, G. Monaco, G. Talarico, M. Vacatello, J.C. Chadwick, A.L. Segre, O. Sudmeijer, Macromolecules 32 (1999) 4173–4182.

[9] N. Cui, Y. Ke, H. Li, Z. Zhang, C. Guo, Z. Lv, Y. Hu, J. Appl. Polym. Sci. 99 (2006) 1399–1404.
[10] J.C. Chadwick, G. Morini, G. Balbontin, I. Camurati, J.J.R. Heere, I. Mingozzi, F. Testoni, Macromol. Chem. Phys. 202 (2001) 1995–2002.
[11] H. Matsuoka, B. Liu, H. Nakatani, M. Terano, Macromol. Rapid Commun. 22 (2001) 326–328.
[12] V. Busico, J.C. Chadwick, R. Cipullo, S. Ronca, G. Talarico, Macromolecules 37 (2004) 7437–7443.
[13] Q. Wang, N. Murayama, B. Liu, M. Terano, Macromol. Chem. Phys. 206 (2005) 961–966.
[14] A.K. Yaluma, P.J.T. Tait, J.C. Chadwick, J. Polym. Sci. A 44 (2006) 1635–1647.
[15] G.D. Bukatov, V.A. Zakharov, Macromol. Chem. Phys. 202 (2001) 2003–2009.
[16] A. Andoni, J.C. Chadwick, H.J.W. Niemantsverdriet, P.C. Thüne, J. Catal. 257 (2008) 81–86.
[17] E. Albizzati, M. Galimberti, Catal. Today 41 (1998) 159–168.
[18] R. Scordamaglia, L. Barino, Macromol. Theory Simul. 7 (1998) 399–405.
[19] L. Barino, R. Scordamaglia, Macromol. Theory Simul. 7 (1998) 407–419.
[20] M. Toto, G. Morini, G. Guerra, P. Corradini, L. Cavallo, Macromolecules 33 (2000) 1134–1140.
[21] M. Boero, M. Parrinello, H. Weiss, S. Hüffer, J. Phys. Chem. A 105 (2001) 5096–5105.
[22] M. Seth, P.M. Margl, T. Zieger, Macromolecules 35 (2002) 7815–7829.
[23] T. Ziegler, M. Seth, Macromolecules 36 (2003) 6613–6623.
[24] Z. Flisak, T. Ziegler, Macromolecules 38 (2005) 9865–9872.
[25] A. Correa, F. Piemontesi, G. Morini, L. Cavallo, Macromolecules 40 (2007) 9181–9189.
[26] M. Boero, M. Parrinello, S. Hüffer, H. Weiss, J. Am. Chem. Soc. 122 (2000) 501–509.
[27] P. Corradini, V. Barone, G. Guerra, Macromolecules 15 (1982) 1242–1245.
[28] G. Monaco, M. Toto, G. Guerra, P. Corradini, L. Cavallo, Macromolecules 33 (2000) 8953–8962.
[29] P. Corradini, G. Guerra, L. Cavallo, Acc. Chem. Res. 37 (2004) 231–241.
[30] J.W. Lee, W.H. Jo, J. Organomet. Chem. 692 (2007) 4639–4646.
[31] L. Brambilla, G. Zerbi, F. Piemontesi, S. Nascetti, G. Morini, J. Mol. Catal. A: Chem. 263 (2007) 103–111.
[32] L. Cavallo, S. Del Piero, J. Ducere, R. Fedele, A. Melchior, G. Morini, F. Piemontesi, M. Tolazzi, J. Phys. Chem. C 111 (2007) 4412–4419.
[33] V. Busico, M. Causà, R. Cipullo, R. Credendino, F. Cutillo, N. Friederichs, R. Lamanna, A. Sergre, V. Van Axel Castelli, J. Phys. Chem. C 112 (2008) 1081–1089.
[34] S.H. Vosko, L. Wilk, M. Nusair, Can. J. Phys. 58 (1980) 1200–1211.
[35] A.D. Becke, Phys. Rev. A 38 (1988) 3098–3100.
[36] J.P. Perdew, Phys. Rev. B 33 (1986) 8822–8824.
[37] C.F. Guerra, J.G. Snijders, G. te Velde, E.J. Baerends, Theor. Chem. Acc. 99 (1998) 391–403.
[38] A.K. Rappe, C.J. Casewit, K.S. Colwell, W.A. Goddard-III, W.M. Skiff, J. Am. Chem. Soc. 114 (1992) 10024–10035.
[39] D.E. Partin, M. O'Keeffe, J. Solid State Chem. 95 (1991) 176–183.
[40] P. Cossee, J. Catal. 3 (1964) 80–88.
[41] E. Arlman, J. Catal. 3 (1964) 89–98.
[42] E. Arlman, P. Cossee, J. Catal. 3 (1964) 99–104.
[43] M. Brookhart, M.L.H. Green, J. Organomet. Chem. 250 (1983) 395–408.
[44] L. Cavallo, G. Guerra, P. Corradini, J. Am. Chem. Soc. 120 (1998) 2428–2436.
[45] J.C.W. Chien, P. Bres, J. Polym. Sci. A 24 (1986) 1967–1988.